*Inorg. Chem.* **2007**, *46*, 10578–10586


# Bimetallic $M^V_2Cu^{II}_3$ (M = Mo, W) Coordination Complexes Based on Octacyanometalates: Structures and Magnetic Variations Tuned by Chelated Tetradentate Macrocyclic Ligands

**Jeong Hak Lim,[†] Young Sin You,[†] Houng Sik Yoo,[†] Jung Hee Yoon,[†] Jae Il Kim,[†] Eui Kwan Koh,[‡] and Chang Seop Hong*,[†]**

*Department of Chemistry, Korea University, Seoul 136-713, Korea, and Nano-Bio System Research Team, Korea Basic Science Institute, Seoul 136-713, Korea*

Received June 25, 2007

Four octacyanometalate-based bimetallic Cu–M (M = Mo, W) assemblies coordinated by tetradentate macrocyclic ligands were prepared via self-assembly process in a stoichiometric ratio of $[M(CN)_8]^{3-}$ and $Cu(macrocycle)^{2+}$ and characterized in terms of structures and magnetic properties. The crystal structures are varied depending on the macrocycles used. The employment of cyclam with no pendant groups produced a one-dimensional chain (**1**) with a rope-ladder pattern, whereas macrocycles with side groups allowed for the formation of two-dimensional honeycomb-like architectures (**2**–**4**). From the crystal structures, the variations in apical Cu–$N_{ax}$ lengths and Cu–$N_{ax}$–$C_{ax}$ angles on the bridging pathways are observed, which arises from the existence of side groups on macrocyclic ligands. The magnetic results reveal that all of the prepared compounds show ferromagnetic couplings between magnetic centers transimitted through CN bridges under the present structural parameters. Comparing the magnetic strength of the Cu–Mo (3d–4d; **2**) and Cu–W (3d–5d; **3**) complexes supports that 3d–5d magnetic coupling is stronger than 3d–4d because the 5d orbital is more diffuse than 4d. The magnetic analyses for **1**–**4** and related complexes tentatively suggest that, when the Cu–$N_{ax}$ distances are long enough, the axial Cu–$N_{ax}$ bond length in the bridging route may be one of the major structural parameters to determine the magnitude of the ferromagnetic exchange coupling.

## Introduction

The construction of new molecule-based magnetic materials has been of high interest because of their potential applications in magnetic devices. To this end, hexacyanometalates $[A(CN)_6]^{m-}$ (A = V, Cr, Mn, Fe) have been frequently utilized to fabricate clusters and extended coordination networks particularly exhibiting slow magnetic relaxation,[1] high $T_C$,[2] and photomagnetic characters.[3] In recent times, octacyanometalates $[B(CN)_8]^{n-}$ (B = Mo, W, Nb, Re) have been successfully employed as useful building blocks to achieve diverse bimetallic magnetic systems.[4] They have merits of the strong magnetic interactions induced by their diffuse 4d/5d orbitals, various geometric structures (dodecahedron, square anitiprism, and bicapped trigonal prism), and photoresponsive properties.[3,4] The combination of the anionic species with paramagnetic metal cations ($Mn^{II}$, $Fe^{II}$, $Co^{II}$, $Ni^{II}$) produced self-assembly of bimetallic entities

* To whom correspondence should be addressed. E-mail: cshong@korea.ac.kr.
[†] Korea University.
[‡] Korea Basic Science Institute.

(1) Berlinguette, C. P.; Vaughn, D.; Cañada-Vilalta, C.; Galán-Mascarós, J. R.; Dunbar, K. R. *Angew. Chem., Int. Ed.* **2003**, *42*, 1523.
(2) Holmes, S. M.; Girolami, G. S. *J. Am. Chem. Soc.* **1999**, *121*, 5593.
(3) (a) Dei, A. *Angew. Chem., Int. Ed.* **2005**, *44*, 1160. (b) Arimoto, Y.; Ohkoshi, S.-i.; Zhong, Z. J.; Seino, H.; Mizobe, Y.; Hashimoto, K. *J. Am. Chem. Soc.* **2003**, *125*, 9240. (c) Herrera, J. M.; Marvaud, V.; Verdaguer, M.; Marrot, J.; Kalisz, M.; Mathonière, C. *Angew. Chem., Int. Ed.* **2004**, *43*, 5468. (d) Ohkoshi, S.-i.; Tokoro, H.; Hozumi, T.; Z, Y.; Hashimoto, K.; Mathonière, C.; Bord, I.; Rombaut, G.; Verlelst, M.; Moulin, C. C. d.; Villain, F. *J. Am. Chem. Soc.* **2006**, *128*, 270. (e) Ohkoshi, S.-i.; Ikeda, S.; Hozumi, T.; Kashiwagi, T.; Hashimoto, K. *J. Am. Chem. Soc.* **2006**, *128*, 5320.
(4) (a) Bennett, M. V.; Long, J. R. *J. Am. Chem. Soc.* **2003**, *125*, 2394. (b) Pradhan, R.; Desplanches, C.; Guionneau, P.; Sutter, J.-P. *Inorg. Chem.* **2003**, *42*, 6607. (c) Withers, J. R.; Li, D.; Jeremy, T.; Ruschman, C.; Parkin, S.; Wang, G.; Yee, G. T.; Holmes, S. M. *Polyhedron* **2007**, *26*, 2353. (d) Kashiwagi, T.; Ohkoshi, S.-i.; Seino, H.; Mizobe, Y.; Hashimoto, K. *J. Am. Chem. Soc.* **2004**, *126*, 5024. (e) Li, D.-f.; Gao, S.; Zheng, L.-m.; Tang, W.-x. *Dalton Trans.* **2002**, 2805. (f) Podgajny, R.; Balanda, M.; Sikora, M.; Borowiec, M.; Spalek, L; Kapusta, C.; Sieklucka, B. *Dalton Trans.* **2006**, 2801. (g) Shores, M. P.; Sokol, J. J.; Long, J. R. *J. Am. Chem. Soc.* **2002**, *124*, 2279. (h) Ruiz, E.; Rodríguez-Fortea, A.; Alvarez, S.; Verdaguer, M. *Chem.—Eur. J.* **2005**, *11*, 2135. (i) Visinescu, D.; Desplanches, C.; Imaz, I.; Bahers, V.; Pradhan, R.; Villamena, F. A.; Guionneau, P.; Sutter, J.-P. *J. Am. Chem. Soc.* **2006**, *128*, 10202.


10.1021/ic701243w CCC: $37.00

Published on Web 11/07/2007

with structures spanning from discrete molecules,[5] one-dimensional (1D) chains,[6] and 2D layers[7] to 3D frameworks.[8] For instance, some of the octacyanometalate-based clusters afforded high ground-state spins exemplified as the bimetallic assembly $[Mn\{Mn(EtOH)_3\}_8\{W(CN)_8\}_6]\cdot 12EtOH$ with a maximum spin state of $S = {}^{39}/_2$ resulting from intracluster antiferromagnetic couplings between nine $Mn^{II}$ ($S_{Mn} = {}^5/_2$) and six $M^V$ ($S_M = {}^1/_2$).[9] The heteropolynuclear cluster containing Co(II) as an anisotropic source displayed the first single-molecule magnet (SMM) properties among the $M'_9M_6$ family with the formula $[M'\{M'(S)_3\}_8\{M(CN)_8\}_6]\cdot xS\cdot yH_2O$ (M = Mo, W; M′ = Mn, Co, Ni; S = MeOH or EtOH).[5,9,10] Moreover, the surface modification of the $Ni_9W_6$ parent molecule by replacing the alcoholic solvent molecules with the bidentate ligand 2,2′-bipyridine yielded the air-stable bipyridine-capped $Ni_9W_6$ cluster ($S = 12$) that has intramolecular antiferromagnetic interactions and shows slow relaxation of the magnetization.[5b,11] Also, high-$T_C$ materials based on octacyanometalates were obtained in $Mn^{II}-W^V$ systems with critical temperatures up to $T_C = 54$ K, $Mn^{II}-Mo^V$ with $T_N = 8$ K, and $Mn^{II}-Nb^{IV}$ with $T_C = 50$ K, where all of the $Mn^{II}$ ions are antiparallel to all the M spins.[4e,7a,8b,12,13]

Octacyanometalate-linked Cu−M (M = Mo, W) bimetallic systems including 1D chain,[14] 2D sheet,[15] and 3D network[16] structures have been actively explored. In view of orbital interactions across the cyanide ligand, it is predicted that the overlap between M d$\pi$ and Cu d$\sigma$ orbitals may give ferromagnetic interactions due to orbital orthogonality.[17] Many examples supportive of the ferromagnetic exchange nature of such bimetallic assemblies have been found in cyano-bridged Cu−M systems.[14−16] However, when the magnetic M d$\pi$ orbital and the Cu $d_{x^2-y^2}$ orbital oriented toward the equatorial plane of tetradentate ligands are involved, elaborate investigations need to be devised in order to evaluate their operating magnetic behaviors. To rationalize the magnetic exchange nature in the latter, fine-tuning of structural environments that affect magnetic properties becomes therefore a challenge. One of the sensible strategies is to choose six-coordinate Cu(II) precursors comprising four equatorial atoms from tetradentate macrocyclic ligands and two apical sites reserved for bridging ligands. Our effort has been to seek a correlation between adjusted structural parameters and resulting magnetic characters by modulating subtle molecular structures that rest on changing side groups on macrocycles.[18]

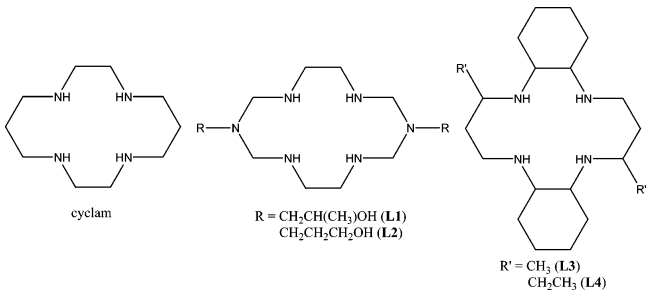


Herein we report the syntheses, crystal structures, and magnetic properties of a 1D rope-ladder chain compound $[Cu(cyclam)]_3[W(CN)_8]_2\cdot 5H_2O$ (**1**·$5H_2O$) bound by cyclam with no side groups and three 2D honeycomb-like systems, $[Cu(L2)]_3[Mo(CN)_8]_2\cdot 10H_2O\cdot 2MeCN$ (**2**·$10H_2O$·2MeCN), $[Cu(L2)]_3[W(CN)_8]_2\cdot 10H_2O\cdot 2MeCN$ (**3**·$10H_2O$·2MeCN), and $[Cu(L3)]_3[W(CN)_8]_2\cdot 2H_2O$ (**4**·$2H_2O$), chelated with tetradentate macrocyclic ligands having pendant groups. They were formed by self-assembling $[M(CN)_8]^{3-}$ (M = Mo, W) and molecular precursors $[Cu(macrocycle)]^{2+}$ in a stoichiometric reaction ratio. The structural parameters of axial $Cu-N_{ax}$ bond length and $Cu-N_{ax}-C_{ax}$ angle are varied by introducing diverse pendant groups on the macrocyclic ligands. Magnetic measurements show that ferromagnetic couplings between Cu(II) and M(V) ions occur through the CN bridges under the given structural features. The magnitude of the observed ferromagnetic exchange is likely to be relevant with the variation of average $\langle d_{Cu-N_{ax}}\rangle$ bond distance rather than the change in average $\langle \angle Cu-N_{ax}-C_{ax}\rangle$ angle.

## Experimental Section

**Reagent.** $(Bu_4N)_3[M(CN)_8]$ (M = Mo, W), $Cu(cyclam)(NO_3)_2$, $[Cu(L2)](ClO_4)_2$, and $[Cu(L3)](ClO_4)_2$ used in the synthesis were

(5) (a) Podgajny, R.; Deaplanches, C.; Sieklucka, B.; Sessoli, R.; Villar, V.; Paulsen, C.; Wernsdorfer, W.; Dromzée, Y.; Verdaguer, M. *Inorg. Chem.* **2002**, *41*, 1323. (b) Bonadio, F.; Gross, M.; Stoeckli-Evans, H.; Decurtins, S. *Inorg. Chem.* **2002**, *41*, 5891. (c) Freedman, D. E.; Bennett, M. V.; Long, J. R. *Dalton Trans.* **2006**, 2829.
(6) (a) Li, D.; Zheng, L.; Zhang, Y.; Huang, J.; Gao, S.; Tang, W. *Inorg. Chem.* **2003**, *42*, 6123. (b) Zhao, H.; Shatruk, M.; Prosvirin, A. V.; Dunbar, K. R. *Chem.−Eur. J.* **2007**, *13*, 6573.
(7) (a) Withers, J. R.; Li, D.; Triplet, J.; Ruschman, C.; Parkin, S.; Wang, G.; Yee, G. T.; Holmes, S. M. *Inorg. Chem.* **2006**, *45*, 4307. (b) Withers, J. R.; Li, D.; Triplet, J.; Ruschman, C.; Parkin, S.; Wang, G.; Yee, G. T.; Holmes, S. M. *Polyhedron* **2007**, *26*, 2353. (c) Podgajny, R.; Balanda, M.; Sikora, M.; Borowiec, M.; Spalek, L.; Kapusta, C.; Sieklucka, B. *Dalton Trans.* **2006**, 2801.
(8) (a) Herrera, J. M.; Bleuzen, A.; Dromzée, Y.; Julve, M.; Lloret, F.; Verdaguer, M. *Inorg. Chem.* **2003**, *42*, 7052. (b) Song, Y.; Ohkoshi, S.-i.; Arimoto, Y.; Seino, H.; Mizobe, Y.; Hashimoto, K. *Inorg. Chem.* **2003**, *42*, 1848.
(9) Zhong, Z. J.; Seino, H.; Mizobe, Y.; Hidai, M.; Fujishima, A.; Ohkoshi, S.-i.; Hashimoto, K. *J. Am. Chem. Soc.* **2000**, *122*, 2952.
(10) Song, Y.; Zhang, P.; Ren, X.-M.; Shen, X.-F.; Li, Y.-Z.; You, X.-Z. *J. Am. Chem. Soc.* **2005**, *127*, 3708.
(11) Lim, J. H.; Yoon, J. H.; Kim, H. C.; Hong, C. S. *Angew. Chem., Int. Ed.* **2006**, *45*, 7424.
(12) Zhong, Z. J.; Seino, H.; Mizobe, Y.; Hidai, M.; Verdaguer, M.; Ohkoshi, S.-i.; Hashimoto, K. *Inorg. Chem.* **2000**, *39*, 5095.
(13) Pilkington, M.; Dercurtins, S. *Chimia* **2000**, *54*, 593.
(14) You, Y. S.; Kim, D.; Do, Y.; Oh, S. J.; Hong, C. S. *Inorg. Chem.* **2004**, *43*, 6899.
(15) (a) Li, D.-f.; Zheng, L.-m.; Wang, X.-y.; Huang, J.; Gao, S.; Tang, W.-x. *Chem. Mater.* **2003**, *15*, 2094. (b) Korzeniak, T.; Stadnicka, K.; Rams, M.; Sieklucka, B. *Inorg. Chem.* **2004**, *43*, 4811. (c) Korzeniak, T.; Stadnicka, K.; Pelka, R.; Balanda, M.; Tomala, K.; Kowalski, K.; Sieklucka, B. *Chem. Commun. (Cambridge)* **2005**, 2939. (d) Podgajny, R.; Korzeniak, T.; Balanda, M.; Wasiutynski, T.; Errington, W.; Kemp, T. J.; Alcock, N. W.; Sieklucka, B. *Chem. Commun. (Cambridge)* **2002**, 1138. (e) Ohkoshi, S.-i.; Arimoto, Y.; Hozumi, T.; Seino, H.; Mizobe, Y.; Hashimoto, K. *Chem. Commun. (Cambridge)* **2003**, 2772. (f) Li, D.-f.; Gao, S.; Zheng, L.-m.; Yu, K.-b.; Tang, W.-x. *New. J. Chem.* **2002**, *26*, 1190.
(16) (a) Li, D. F.; Gao, S.; Zheng, L.-M.; Sun, W.-Y.; Okamura, T.-a.; Ueyama, N.; Tang, W.-X. *New J. Chem.* **2002**, *26*, 485. (b) Ohkoshi, S.-i.; Tsunobuchi, Y.; Takahashi, H.; Hozumi, T.; Shiro, M.; Hashimoto, K. *J. Am. Chem. Soc.* **2007**, *129*, 3084. (c) Chen, F.-T.; Li, D.-F.; Gao, S.; Wang, X.-Y.; Li, Y.-Z.; Zheng, L.-M.; Tang, W.-X. *Dalton Trans.* **2003**, 3283.
(17) Kahn, O. *Molecular Magnetism*; VCH: Weinheim, Germany, 1993.
(18) (a) You, Y. S.; Yoon, J. H.; Kim, J. H.; Kim, H. C.; Hong, C. S. *Inorg. Chem.* **2005**, *44*, 7063. (b) Lim, J. H.; Kang, J. S.; Kim, H. C.; Koh, E. K.; Hong, C. S. *Inorg. Chem.* **2006**, *45*, 7821.

**Table 1.** Crystallographic Data for **1**−**4**

| | **1**·5H$_2$O | **2**·10H$_2$O·2MeCN | **3**·10H$_2$O·2MeCN | **4**·2H$_2$O |
|---|---|---|---|---|
| formula | $C_{46}H_{82}Cu_3N_{28}O_5W_2$ | $C_{62}H_{126}Cu_3Mo_2N_{36}O_{16}$ | $C_{62}H_{126}Cu_3W_2N_{36}O_{16}$ | $C_{76}H_{122}Cu_3N_{28}OW_2$ |
| Fw | 1665.72 | 2014.49 | 2190.31 | 2002.34 |
| cryst syst | triclinic | triclinic | triclinic | triclinic |
| space group | $P\bar{1}$ | $P\bar{1}$ | $P\bar{1}$ | $P\bar{1}$ |
| temp (K) | 293 | 130 | 130 | 293 |
| $a$ (Å) | 8.9255(11) | 9.8095(2) | 9.8329(2) | 16.2688(3) |
| $b$ (Å) | 10.0938(13) | 15.5889(3) | 15.5828(4) | 18.7141(4) |
| $c$ (Å) | 19.549(3) | 16.0992(4) | 16.0557(4) | 19.1070(4) |
| α (deg) | 78.342(5) | 70.2270(10) | 70.3950(10) | 116.0870(10) |
| $\beta$ (deg) | 83.074(5) | 85.2760(10) | 85.1500(10) | 111.5880(10) |
| $\gamma$ (deg) | 69.472(5) | 85.9670(10) | 85.8310(10) | 92.1490(10) |
| $V$ (Å$^3$) | 1613.0(4) | 2306.49(9) | 2306.63(9) | 4717.77(17) |
| Z | 1 | 1 | 1 | 2 |
| $d_{calc}$ (g cm$^{-3}$) | 1.715 | 1.452 | 1.577 | 1.410 |
| $\mu$ (mm$^{-1}$) | 4.590 | 1.021 | 3.241 | 3.149 |
| $F$(000) | 829 | 1051 | 1113 | 2034 |
| $\theta$ range (deg) | 1.07−28.28 | 1.35−28.30 | 1.35−28.28 | 1.25−28.35 |
| reflns collected | 21 064 | 38 386 | 31 188 | 78 179 |
| unique reflns | 7 570 | 11 288 | 10 815 | 23 122 |
| no. of params | 380 | 517 | 515 | 1000 |
| R1 [a] [$I > 2\sigma(I)$] | 0.0693 | 0.0471 | 0.0376 | 0.0439 |
| wR2 [b] [$I > 2\sigma(I)$] | 0.1662 | 0.1188 | 0.0821 | 0.0960 |

[a] $R1 = \sum||F_o| - |F_c||/\sum|F_c|$. [b] $wR2 = [\sum w(F_o^2 - F_c^2)^2/\sum w(F_o^2)^2]^{1/2}$.

prepared according to the literature procedures.[19−22] All chemicals and solvents in the synthesis were of reagent grade and used as received. All manipulations were performed under aerobic conditions.

**Synthesis.** ***Caution!*** *Perchlorate salts of metal compounds with organic ligands are potentially explosive. Only small amounts of material should be cautiously handled.*

**[Cu(cyclam)]$_3$[W(CN)$_8$]$_2$·5H$_2$O (1·5H$_2$O).** To an aqueous solution of Cu(cyclam)(NO$_3$)$_2$ (0.15 mmol) was added a methanolic solution of (Bu$_4$N)$_3$[W(CN)$_8$] (0.10 mmol) with stirring. Immediately, crystalline product was precipitated. Pink-brown plate single crystals suitable for X-ray were obtained by layering the two solutions. Yield: 85%. Anal. Calcd for $C_{46}H_{82}Cu_3N_{28}O_5W_2$: C, 33.2; H, 4.96; N, 23.6. Found: C, 33.4; H, 4.73; N, 23.2.

**[Cu(L2)]$_3$[Mo(CN)$_8$]$_2$·10H$_2$O·2MeCN (2·10H$_2$O·2MeCN).** (Bu$_4$N)[Mo(CN)$_8$] (0.10 mmol) in MeCN (10 mL) was added to [Cu(L2)](ClO$_4$)$_2$ (0.15 mmol) dissolved in a 10 mL mixed solvent of MeCN/H$_2$O (10:1). The filtered solution was left undisturbed in the dark, forming red crystals in a yield of 35%. The dried solid was analyzed as **2**·9H$_2$O·2MeCN. Anal. Calcd for $C_{62}H_{124}Cu_3Mo_2N_{36}O_{15}$: C, 37.3; H, 6.26; N, 25.3. Found: C, 37.6; H, 6.19; N, 25.1.

**[Cu(L2)]$_3$[W(CN)$_8$]$_2$·10H$_2$O·2MeCN (3·10H$_2$O·2MeCN).** A methanolic solution of (Bu$_4$N)$_3$[W(CN)$_8$] (0.10 mmol) was added to [Cu(L2)](ClO$_4$)$_2$ (0.15 mmol) dissolved in MeCN/H$_2$O (5:1). After stirring for a few minutes the resulting solution was filtered. The filtrate was allowed to stand undisturbed in the dark, giving red crystals in a yield of 63%. The dried solid was analyzed as **3**·10H$_2$O. Anal. Calcd for $C_{58}H_{120}Cu_3N_{34}O_{16}W_2$: C, 33.0; H, 5.74; N, 22.6. Found: C, 33.1; H, 5.31; N, 22.2.

**[Cu(L3)]$_3$[W(CN)$_8$]$_2$·2H$_2$O (4·2H$_2$O).** [Cu(L3)](ClO$_4$)$_2$ in MeCN/H$_2$O (2:1) was mixed with (Bu$_4$N)$_3$[W(CN)$_8$] (0.10 mmol) in MeOH, giving a violet solution. The filtered solution was left without perturbation for several days, producing violet crystals in a yield of 64%. Anal. Calcd for $C_{76}H_{122}Cu_3N_{28}OW_2$: C, 45.6; H, 6.14; N, 19.6. Found: C, 45.8; H, 6.01; N, 19.7.

**Physical Measurements.** Elemental analyses for C, H, and N were performed at the Elemental Analysis Service Center of Sogang University. Infrared spectra were obtained from KBr pellets with a Bomen MB-104 spectrometer. Magnetic susceptibilities for **1**−**4** were carried out using a Quantum Design MPMS-7 SQUID susceptometer at Seoul Branch, KBSI. Diamagnetic corrections of **1**−**4** were estimated from Pascal's Tables.

**Crystallographic Structure Determination.** X-ray data for **1**−**4** were collected on a Bruker SMART APEXII diffractometer equipped with graphite monochromated Mo Kα radiation ($\lambda$ = 0.710 73 Å). Preliminary orientation matrix and cell parameters were determined from three sets of $\omega$ scans at different starting angles. Data frames were obtained at scan intervals of 0.5° with an exposure time of 10 s/frame. The reflection data were corrected for Lorentz and polarization factors. Absorption corrections were carried out using SADABS.[23] The structures were solved by direct methods and refined by full-matrix least-squares analysis using anisotropic thermal parameters for non-hydrogen atoms with the SHELXTL program.[24] For the asymmetric unit of **2** and **3**, one MeCN was disordered and could not be modeled properly. The SQUEEZE routine of the PLATON program was employed to calculate the disorder area of the solvent molecule and get rid of its contribution to the whole intensity data. The oxygen atom of the pendant group on L2 in **3** was disordered over two sites (O3A and O3B) and refined with an occupancy factor of 0.65:0.35. All hydrogen atoms except for hydrogens bound to water molecules and the carbon atom (C27) attached to disordered oxygen atoms in **3** were calculated at idealized positions and refined with the riding models. Crystallographic data and the details of data collection are listed in Table 1.

## Results and Discussion

**Synthesis and Characterization.** The molecular building units, anionic [M(CN)$_8$]$^{3-}$ (M = Mo, W) and cationic [Cu(L)]$^{2+}$ (L = tetradentate macrocyclic ligand) were self-assembled in a 2:3 stoichiometric ratio to yield neutral M$_2$Cu$_3$

(19) Pribush, R. A.; Archer, R. D. *Inorg. Chem.* **1974**, *13*, 2556.
(20) Clay, R. M.; Steele, W. V. *Inorg. Chem.* **1980**, *19*, 2414.
(21) Suh, M. P.; Shim, B. Y.; Yoon, T.-S. *Inorg. Chem.* **1994**, *33*, 5509.
(22) Kang, S.-G.; Kweon, J. K.; Jung, S.-K. *Bull. Korean Chem. Soc.* **1991**, *12*, 483.
(23) Sheldrick, G. M. *SADABS, A Program for Area Detector Absorption Corrections*; University of Göttingen: Göttingen, Germany, 1994.
(24) Sheldrick, G. M. *SHELXTL*, version 5; Bruker AXS: Madison, WI, 1995.

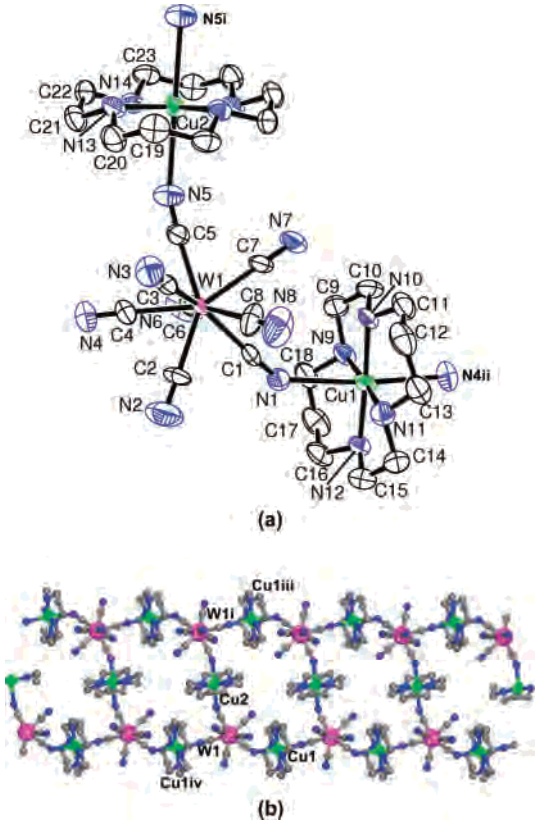


**Figure 1.** (a) ORTEP diagram of **1** with the asymmetric unit and symmetry-related atoms along with the atom-labeling scheme. (b) Extended 1D chain structure. Symmetry codes: i = $-x$, $2-y$, $-z$; ii = $1+x$, $-1+y$, $z$; iii = $1-x$, $1-y$, $-z$; iv = $-1+x$, $1+y$, $z$.

complexes. The reaction progresses were checked from the IR spectra by the absence of a strong NO stretching band of $NO_3^-$ at 1385 vs $cm^{-1}$ for Cu(cyclam)$(NO_3)_2$, strong multiple peaks of the Cl−O vibrations around 1078 vs $cm^{-1}$ for [Cu(L2)]$(ClO_4)_2$, and 1091 vs $cm^{-1}$ for [Cu(L3)]$(ClO_4)_2$. The broad bands centered at 3443 s (**1**), 3436 s (**2**), 3419 s (**3**), and 3487 s $cm^{-1}$ (**4**) are visible, which can be attributed to hydrogen bonding of lattice water molecules and/or hydroxyl groups on L2. For secondary amines, NH stretchings appear at 3259 m, 3232 s, 3209 m, and 3169 m $cm^{-1}$ for **1**; 3255 m, 3228 m, and 3171 m $cm^{-1}$ for **2**; 3259 m and 3228 m $cm^{-1}$ for **3**; and 3240 s and 3169 m (sh) $cm^{-1}$ for **4**. The advent of more than two peaks for the secondary NH groups reveals that hydrogen bonds are involved. The characteristic CN stretching vibrations are positioned at 2166 w, 2154 m, 2147 m, and 2139 m $cm^{-1}$ for **1**; 2143 m $cm^{-1}$ for **2**; 2144 m and 2137 m $cm^{-1}$ for **3**; and 2145 m $cm^{-1}$ for **4**. The shift of peaks toward higher frequencies based on the reference CN peaks centered at 2140 m and 2123 m $cm^{-1}$ for $(Bu_4N)_3Mo(CN)_8$ and 2141 m, 2130 m, and 2123 m (sh) $cm^{-1}$ for $(Bu_4N)_3W(CN)_8$ suggests the existence of bridging CN ligands.

**Description of the Structures.** Compound **1** is shown in Figure 1a with the atom-labeling scheme. The W center adopts a distorted square antiprism consisting of eight CN groups with an average W−C bond length of 2.163(10) Å and a maximum deviation of the W−C−N angle from linearity being 5.6°. Three among eight CN groups are bridged to adjacent Cu(II) ions as expected from the IR data. Each Cu atom is situated in a distorted octahedral geometry. For the Cu center, the basal $N_4$ plane from cylam provides an average Cu−$N_{eq}$ bond distance of 2.019(10) Å, while the axial positions are filled by two N atoms from bridging CN units with elongated lengths of Cu1−N1 = 2.698(10) Å, Cu1−$N4^{ii}$ = 2.510(10) Å (ii = $1+x$, $-1+y$, $z$), and Cu2−N5 = 2.556(10) Å. These significant structural distortions are definitely characteristic of an octahedral Cu(II) ion, which is due to the Jahn−Teller effect. The angles between the Cu ions and the surrounding CN bridges are 143.0(7)° for Cu1−N1−C1, 157.1(8)° for $Cu1^{iv}$−N4−C4 (iv = $-1+x$, $1+y$, $z$), and 157.1(9)° for Cu2−N5−C5. The structural parameters of the axial Cu−NC units in **1** are quite similar to the corresponding ones in the $Cu_3Mo_2$ analogue.[14] Many hydrogen bonds are formed among lattice water molecules and unbound CN groups of $[W(CN)_8]^{3-}$ in the range of 2.908−3.154 Å. The secondary NH moieties on cyclam also have hydrogen bonding to oxygen atoms from lattice water molecules with distances less than 3.128 Å.

The overall structural view in Figure 1b can be described as a 2,3 ladderlike chain.[25] This 1D structural type is also found in hexacyanometalate-based 3d−3d bimetallic systems $[Ni(en)_2]_3[M'(CN)_6]_2\cdot 2H_2O$ (M′ = Cr, Mn, Fe, Co; en = ethylenediamine)[26] and the octacyanometalate-based 3d−4d assembly $[Cu(cyclam)]_3[Mo(CN)_8]_2\cdot 5H_2O$.[14] In a chain, the W−Cu distances via the CN linkage are 5.6999(15) Å for W1−Cu1, 5.7156(8) Å for W1−Cu2, and 5.7447(15) Å for W1−$Cu1^{iv}$. The shortest interchain separations are 7.892 Å for Cu−Cu, 7.540 Å for Cu−W, and 8.925 Å for W−W.

Figures 2a and 3a illustrate the molecular views of **2** and **3** exhibiting the selected atom-labeling schemes. Compounds **2** and **3** are isostructural and crystallize in the triclinic system with space group $P\bar{1}$. The $[M(CN)_8]^{3-}$ (M = Mo(**2**), W(**3**)) anion acts as a molecular bridge to link neighboring cationic $[Cu(L2)]^{2+}$ centers. The geometry around M can be viewed as an irregular square antiprism. The basic structural parameters of average M−C distances and maximum deviations of M−C−N from 180° correspond to 2.161(5) Å, 4.7° for **2** and 2.170(5) Å, 4.2° for **3**, respectively. They are in the normal range of ocatacyanometalate-based bimetallic systems.[5−18] The M centers are linked to the $[Cu(L2)]^{2+}$ moieties through three bridging CN ligands of $[M(CN)_8]^{3-}$ with distances of 5.5003(3) Å for Mo1−Cu1, 5.4647(3) Å for Mo1−Cu2, and 5.5483(3) Å for Mo1−Cu3 and 5.4986(2) Å for W1−Cu1, 5.4583(2) Å for W1−Cu2, and 5.5575(2) Å for W1−Cu3. Each Cu atom exhibits a distorted octahedral environment surrounded by four nitrogen atoms from the macrocyclic ligand L2 and two nitrogen atoms from CN bridges of octacyanometalates. The four nitrogens from L2 form the equatorial plane with average Cu−$N_{eq}$ lengths of 2.016(9) Å for **2** and 2.019(10) Å for **3**. The two nitrogens of different bridging CN ligands constitute the apical

(25) Černák, J.; Orendáč, M.; Potočňák, I.; Chomič, J.; Orendáčová, A.; Skoršepa, J.; Feher, A. *Coord. Chem. Rev.* **2002**, *224*, 51.
(26) (a) Ohba, M.; Maruono, N.; Okawa, H.; Enoki, T.; Latour, J.-M. *J. Am. Chem. Soc.* **1994**, *116*, 11566. (b) Ohba, M.; Fukita, N.; Okawa, H. *J. Chem. Soc., Dalton Trans.* **1997**, 1733.

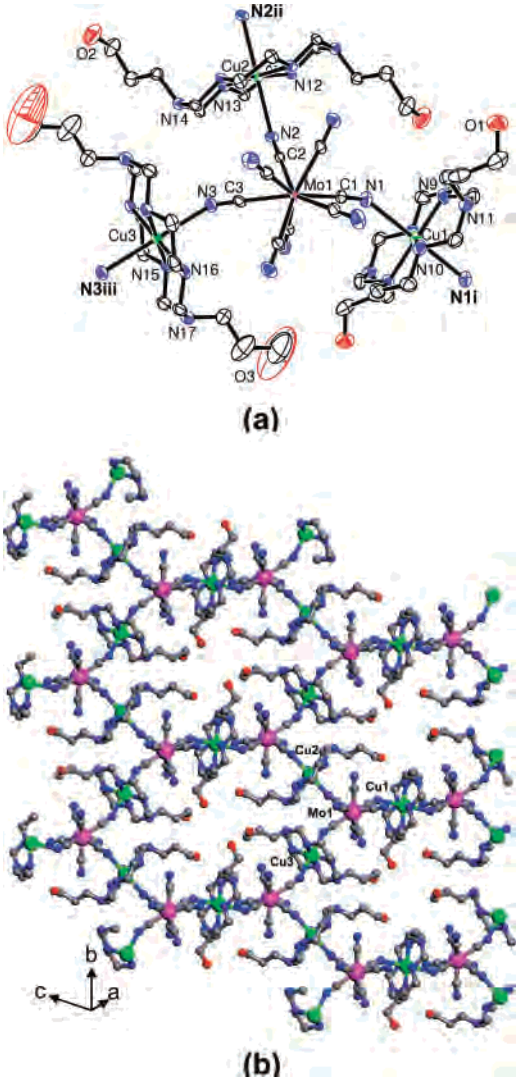


**Figure 2.** (a) ORTEP diagram of **2** with the asymmetric unit and symmetry-related atoms along with the selected atom-labeling scheme. (b) Extended 2D layered structure. Symmetry codes: i = 1 − *x*, 1 − *y*, −*z*; ii = −*x*, 1 − *y*, 1 − *z*; iii = −*x*, −*y*, 1 − *z*.

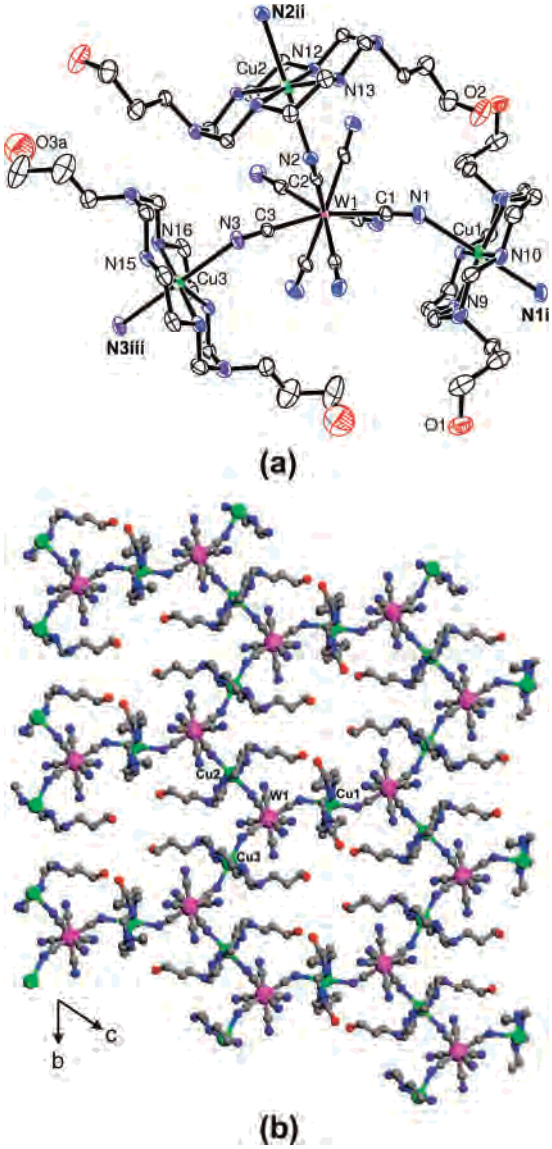


**Figure 3.** (a) ORTEP diagram of **3** with the asymmetric unit and symmetry-related atoms along with the selected atom-labeling scheme. (b) Extended 2D honeycomb-like structure. Symmetry codes: i = 1 − *x*, 1 − *y*, 2 − *z*; ii = 2 − *x*, 1 − *y*, 1 − *z*; iii = 2 − *x*, 2 − *y*, 1 − *z*.

positions, and the elongated distances for **2** and **3** are quite similar, 2.554(3) and 2.544(4) Å for Cu1−N1, 2.507(3) and 2.506(3) Å for Cu2−N2, and 2.494(3) and 2.494(4) Å for Cu3−N3. Therefore, typical Jahn−Teller distortions are essentially observed in the Cu(II) centers. Another structural parameter of the Cu−N−C angle in **2** is equal to 141.3(5)° for Cu1−N1−C1, 142.1(3)° for Cu2−N2−C2, and 145.9(3)° for Cu3−N3−C3. The angles of **3** are almost the same as those of **2**, 141.1(4)° for Cu1−N1−C1, 142.2(3)° for Cu2−N2−C2, and 145.5(3)° for Cu3−N3−C3. It is noted that the presence of the side groups on L2 in **2** and **3** give rise to acuter Cu−NC angles than those in **1** on the basis of cyclam with no pendant groups. This is clearly associated with the pendant groups (-$CH_2CH_2CH_2OH$) on the L2 ligands, which serve as bulkiness to provide a steric hindrance that influences structural patterns around the corresponding Cu atoms (Figure S1). The bond lengths (*d*) and angles (α) between Cu and bridging CN units in **2** and **3** chelated with L2 are fairly homogeneous in view of small variations in length ($\Delta d$ = 0.06 Å) and angle (Δα = 4.6° for **2** and 4.4° for **3**). These parameters can be compared with Cu−M bimetallic systems ligated by different macrocycles, cyclam in **1** ($\Delta d$ = 0.188 Å; Δα = 14.1°), L1 ($\Delta d$ = 0.035 Å; Δα = 22.1° for Cu−Mo and 21.8° for Cu−W),[18a] and L3 in **4** ($\Delta d$ = 0.385 Å; Δα = 15°). This appreciable disparity arises from the fact that, among them, the pendant groups (-$CH_2CH_2CH_2OH$) of the L2 ligands in **2** and **3** are arranged most regularly throughout the crystal lattice.

The hydroxyl groups participate in hydrogen bonding to lattice water molecules and the secondary amines of L2. Additionally, the amines on L2 are responsible for hydrogen bonds with nonbridged CN groups of $[M(CN)_8]^{3-}$. There are also hydrogen bonds among some of lattice water molecules. These hydrogen bonds originating from the hydroxyl groups on the pendant could play a role in stabilizing current crystal structures because no crystalline products were isolated using

methyl or ethyl side groups only instead of the OH containing pendant groups on the macrocycles.

As seen in Figures 2b and 3b, the extended 2D honeycomb-like sheets are generated by $[M(CN)_8]^{3-}$ anions as corners and $[Cu(L2)]^{2+}$ cations as edges of a hexagon. In the hexagon, the edge distances are in the range of 10.929−11.097 Å for **2** and 10.917−11.115 Å for **3** and the diagonal distances in the range of 16.522−25.141 Å for **2** and 16.460−25.134 Å for **3**. The 2D sheet structures are well-illustrated in the side views of the layers giving the shortest separations of 9.809 Å for Mo−Mo and Cu−Cu, 7.894 Å for Mo−Cu, and 9.833 Å for W−W and Cu−Cu, 7.897 Å for W−Cu (Figure S2 of the Supporting Information).

For **4**, there are two W atoms (W1 and W2) with full occupancy and six Cu atoms with half-occupancy in the asymmetric unit, producing a 2D layered structure composed of two different sheets, the W1 layer and the W2 layer (Figure S3 of the Supporting Information). The crystal structure of one type of the $Cu_{1.5}W$ subunits is displayed in Figure 4a with the selected atom-labeling scheme. The central geometry of the W atom coordinated by eight CN groups is distorted dodecahedral. The average W−C lengths are 2.157(12) Å for W1 and 2.170(10) Å for W2. The W−C−N angles remain nearly linear with maximum deviations from linearity of 3.7° for W1 and 5.4° for W2. Each Cu atom in a distorted octahedral environment shows the typical Jahn−Teller effect judged by a substantial axial elongation. The mean $Cu-N_{eq}$ distance is 2.04(2) Å. For W1, the long apical Cu−N lengths are 2.371(6) Å for Cu1−N5, 2.376(5) Å for Cu2−N6, and 2.423(5) Å for Cu3−N1, while the $Cu-N_{ax}$ lengths for the W2 moiety are 2.460(5) Å for Cu4−N21, 2.641(5) Å for Cu5−N15, and 2.756(6) Å for Cu6−N17. The Cu−N−C angles are 135.7(5)° for Cu1−N5−C5, 146.9(4)° for Cu2−N6−C6, 150.7(5)° for Cu3−N1−C1, 143.4(6)° for Cu4−N21−C45, 143.5(5)° for Cu5−N15−C39, and 138.4(5)° for Cu6−N17−C41. The W1-related structural parameters have smaller $Cu-N_{ax}$ bond lengths and larger $Cu-N_{ax}-C_{ax}$ angles than the W2 case. It is worthy of mentioning that, among all compounds prepared with tetradente macrocyclic ligands, compound **4** has the smallest $Cu-N_{ax}$ length of 2.371(6) Å, which would affect overall magnetic strength through CN ligands. The bending of the $Cu-N_{ax}-C_{ax}$ angle is caused by the presence of both the methyl side groups (C28, C32) and the cyclohexyl group (C16, C17, C18, and symmetry-generated three C atoms). Particularly, the cyclohexyl group on L3 behaves as a bulky side group to engender a steric congestion to the coordination sphere around Cu1. This leads to the observed structural consequences of the short $Cu-N_{ax}$ bond length and acute $Cu-N_{ax}-C_{ax}$ angle in a W1 layer (Figure S4 of the Supporting Information). The complicated hydrogen bonds are evident among noncoordinated CN groups, secondary amines on L3, and lattice water molecules.

As depicted in Figure 4b, three CN groups of $[W(CN)_8]^{3-}$ bridge cationic $[Cu(L3)]^{2+}$ units, generating a 2D honeycomb-like structure. The metal−metal distances are 5.2514(2) Å for W1−Cu1, 5.4493(2) Å for W1−Cu2, 5.5438(2) Å for W1−Cu3, 5.4941(2) Å for W2−Cu4, 5.6189(2) Å for W2−Cu5, and 5.6527(2) Å for W2−Cu6. A hexagon in the W1 layer has edge distances spanning from 10.503 to 11.087 Å and diagonal distances from 18.526 to 25.156 Å, while in case of the W2 layer edge distances in a hexagon range from 10.988 to 11.305 Å and diagonal distances from 18.735 to 25.195 Å. The shortest interlayer distances are 8.499 Å for W−W, 7.727 Å for W−Cu, and 9.357 Å for Cu−Cu.

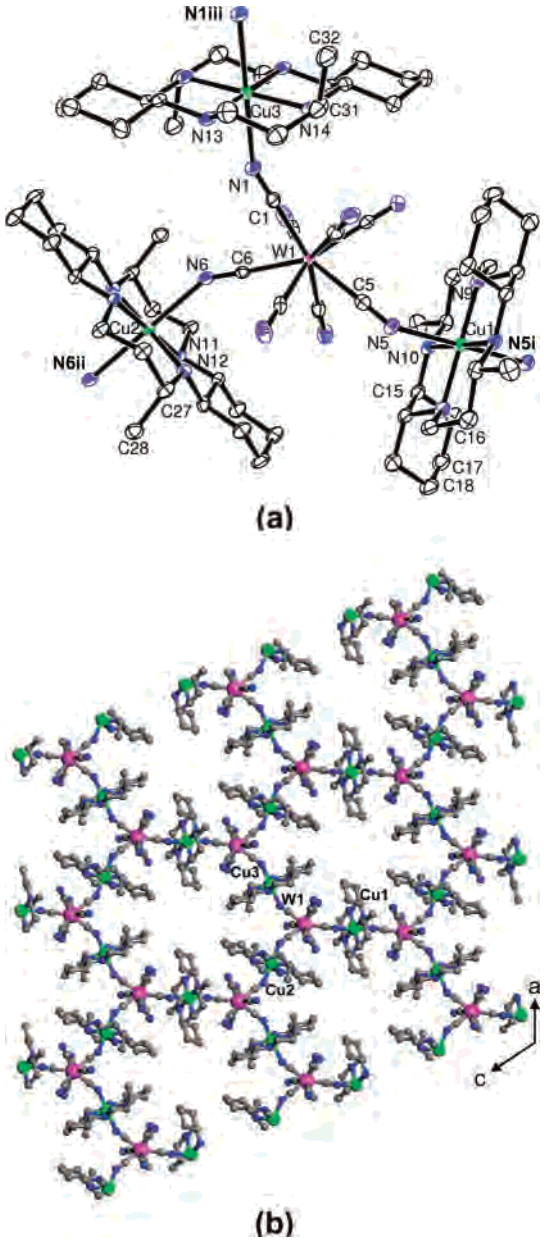


**Figure 4.** (a) ORTEP diagram of **4** with the asymmetric unit and symmetry-related atoms along with the selected atom-labeling scheme. (b) Extended 2D sheet structure. Symmetry codes: i = $-x$, $1-y$, $-z$; ii = $-x$, $1-y$, $1-z$; iii = $1-x$, $1-y$, $1-z$.

**Magnetic Properties.** The temperature dependence of the magnetic susceptibility data for **1** collected at 5000 G in the temperature range of 1.9−300 K was plotted in Figure 5a. The $\chi_m T$ value of 2.00 $cm^3$ K $mol^{-1}$ is slightly larger than the spin-only one (1.88 $cm^3$ K $mol^{-1}$) anticipated from noninteracting two W(V) ($S_W = {}^1/_2$) and three Cu(II) ($S_{Cu} = {}^1/_2$) ions. Decreasing the temperature causes $\chi_m T$ to go on a slow rise and then increase sharply, reaching a maximum value of 2.21 $cm^3$ K $mol^{-1}$ at 6 K. This behavior suggests

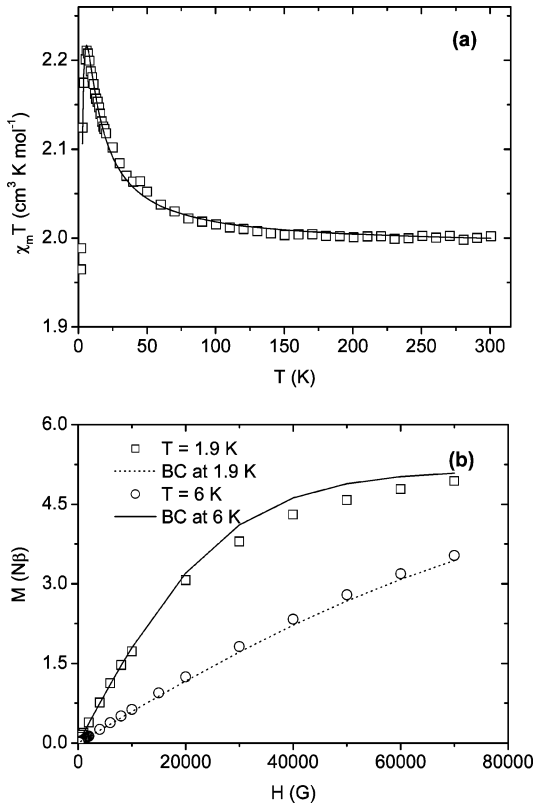


**Figure 5.** (a) Plot of $\chi_m T$ vs $T$ for **1**. The solid line shows the best theoretical fit. (b) Field dependence of the magnetization per $Cu_3W_2$. The Brillouin curves (BC) for the independent three Cu(II) and two W(V) ions are given at 1.9 and 6 K.

the presence of intrachain ferromagnetic interactions. Below the cusp temperature, $\chi_m T$ drops drastically to 1.97 cm$^3$ K mol$^{-1}$ at 1.9 K, suggesting that interchain antiferromagnetic couplings are operating. The magnetic data at $T > 6$ K obey the Curie−Weiss law, resulting in $C = 2.03$ cm$^3$ K mol$^{-1}$ and $\theta = 1.54$ K. The positive Weiss constant ($\theta$) means that adjacent Cu(II) and W(V) centers are ferromagnetically interacted.

To examine the detailed magnetic nature between magnetic centers, Cu(II) and W(V), the structural parameters relevant with the bridging pathways were inspected. The Cu2−N5−C5 and Cu1$^{iv}$−N4−C4 bridging routes retain the similar bond length differing by 0.046 Å and the angle by 0°. The other route of Cu1−N1−C1 is totally different from the aforementioned routes because the gap occurs by 0.142 Å in length and 14.1° in angle. On the basis of the structural feature, we assumed that the former routes transmit stronger magnetic couplings than the latter.[27] Therefore, a proper approximate magnetic model is taken to consider the pentanuclear subunit Cu1$^{iii}$−W1$^{i}$−Cu2−W1−Cu1$^{iv}$ with the spin Hamiltonian $\mathbf{H} = -J_p(S_{Cu1iii}S_{W1i} + S_{W1i}S_{Cu2} + S_{Cu2}S_{W1} + S_{W1}S_{Cu1iv}) + g\beta H(S_{Cu1iii} + S_{W1i} + S_{Cu2} + S_{W1} + S_{Cu1iv})$, where the symmetry codes are defined in the caption of Figure 1. Using the Van Vleck formula the exact expression of the susceptibility of the pentameric unit ($\chi_p$) can be generated (see the Supporting Information). As schematized

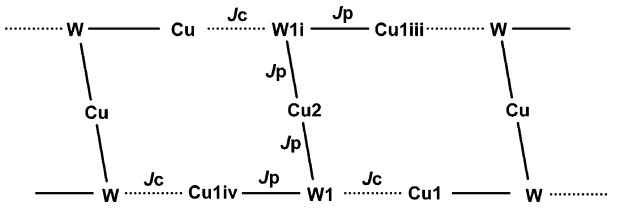


**Figure 6.** Schematic representation of magnetic exchange couplings in **1**. The solid lines stand for intrapentamer interactions ($J_p$) and the dotted ones for interpentamer interactions ($J_c$).

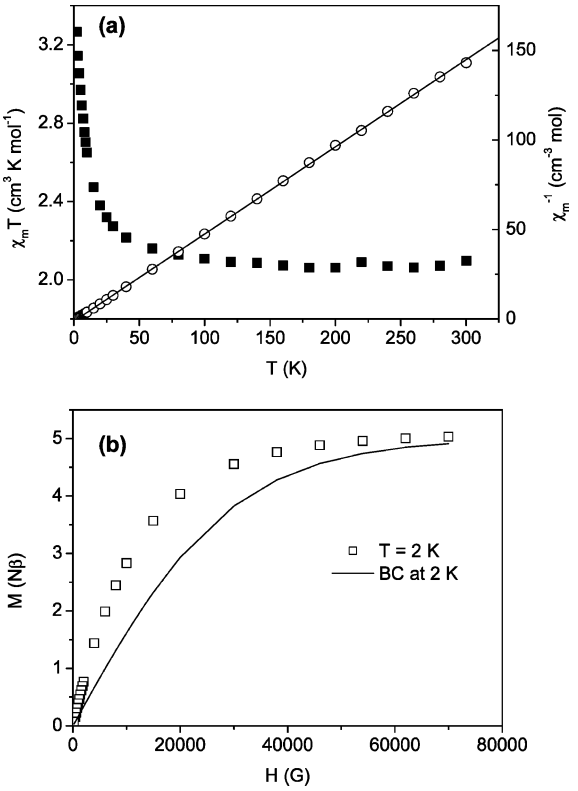


**Figure 7.** (a) Plots of $\chi_m T$ and $\chi_m^{-1}$ vs $T$ for **2**. The solid line presents the Curie−Weiss fit in the high-temperature region. (b) Field dependence of the magnetization per $Cu_3Mo_2$ at 2 K. The Brillouin curve (BC) for the independent three Cu(II) and two Mo(V) ions is shown at 2 K.

in Figure 6, we employed an infinite chain model by regarding the pentamer as a classical spin ($S_p$):[28]

$$\chi_p = (Ng^2\beta^2/3kT)S_p(S_p + 1) \quad (1)$$

$$\chi_c = [Ng^2\beta^2S_p(S_p + 1)/3kT][(1 + u)/(1 - u)] \quad (2)$$

where $u = \coth(J_cS_p(S_p + 1)/kT) - kT/J_cS_p(S_p + 1)$.

The molecular field approximation, represented as $\chi_m = \chi_c/[1 - zJ'\chi_c/Ng^2\beta^2]$, is incorporated into the magnetic model for the chain of the pentamers to take into account interchain magnetic interactions. A magnetic fit of the modified eq 2 to the experimental data provides $g = 2.06$, $J_p = 4.20$ cm$^{-1}$, $J_c = 0.02$ cm$^{-1}$, and $zJ' = -0.57$ cm$^{-1}$. Assuming $J_c = 0$, the obtained parameters are $g = 2.06$, $J_p = 4.20$ cm$^{-1}$, and $zJ' = -0.53$ cm$^{-1}$. Since the $J_c$ value is much smaller than $zJ'$ and close to zero, the magnetic exchange coupling via

(27) Kou, H.-Z.; Zhou, B. C.; Liao, D.-Z.; Wang, R.-J.; Li, Y. *Inorg. Chem.* **2002**, *41*, 6887.

(28) Kou, H.-Z.; Zhou, B. C.; Gao, S.; Liao, D.-Z.; Wang, R.-J. *Inorg. Chem.* **2003**, *42*, 5604.

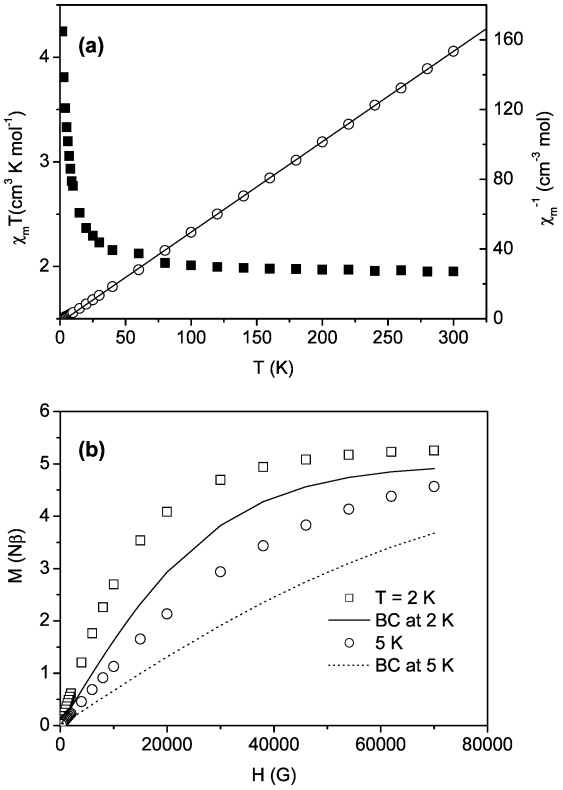


**Figure 8.** (a) Plots of $\chi_m T$ and $\chi_m^{-1}$ vs $T$ for **3**. The solid line represents the Curie−Weiss fit in the high-temperature region. (b) Field dependence of the magnetization per $Cu_3W_2$ at 2 and 5 K. The Brillouin curves (BC) for the independent three Cu(II) and two W(V) ions are given at 2 and 5 K.

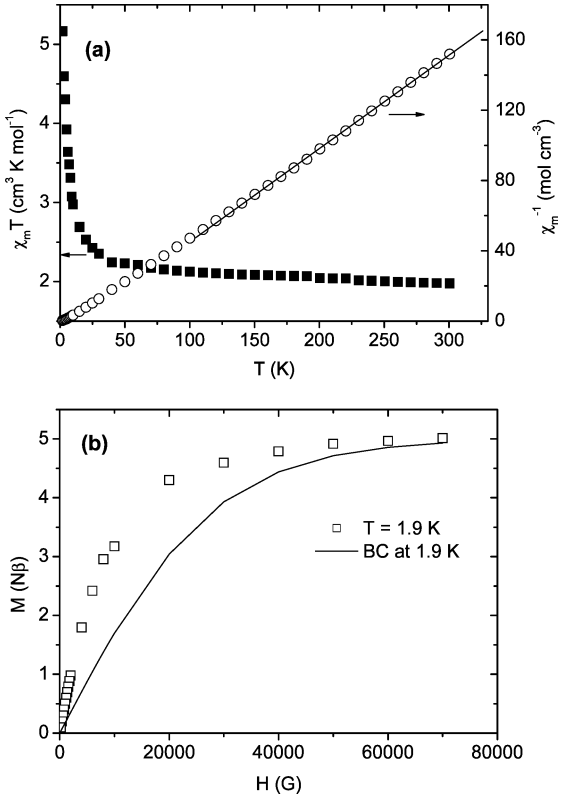


**Figure 9.** (a) Plots of $\chi_m T$ and $\chi_m^{-1}$ vs $T$ for **4**. The solid line denotes the Curie−Weiss fit. (b) Field dependence of the magnetization per $Cu_3W_2$ at 1.9 K. The Brillouin curve (BC) for the independent three Cu(II) and two W(V) ions is given at 1.9 K.

the Cu1−N1−C1 route could be negligible. The observed intrapentamer coupling constant ($J_p$) supports the existence of ferromagnetic interactions between Cu(II) and W(V) in the pentameric unit. The magnitude of $J_p$ in **1** is larger than that in the Cu−Mo chain system, demonstrating that the 5d orbital on W mediates stronger magnetic interactions than the 4d orbital on Mo.[4i,14] The field dependence of magnetization at 1.9 and 6 K is plotted in Figure 5b. The magnetization becomes saturated at 4.94 $N\beta$ in 7 T, which is slightly smaller than the Brillouin curve for noninteracting three Cu(II) and two W(V) spins with $g = 2.06$ at 1.9 K. This behavior is consistent with the $\chi_m T(T)$ data at 1.9 K because the $\chi_m T$ value at 1.9 K is lower than the value at 300 K. The data points at the peak temperature of 6 K lie higher than the theoretical curve, confirming the presence of the dominant ferromagnetic arrangement at that temperature.

The cryomagnetic data for **2** and **3** measured at 1000 G in the temperature range 2−300 K were shown in Figures 7a and 8a. The $\chi_m T$ values at 300 K are 2.09 cm$^3$ K mol$^{-1}$ for **2** and 1.95 cm$^3$ K mol$^{-1}$ for **3**, which are similar to the theoretical value expected for independent two M(V) (M = Mo, W; $S_M = {}^1/_2$) and three Cu(II) ($S_{Cu} = {}^1/_2$) spins. The gradual increase in $\chi_m T$ supports ferromagnetic interactions between M(V) and Cu(II) spins through the CN linkage. The inverse magnetic susceptibilities were fitted with the Curie−Weiss law, affording magnetic parameters of $C = 2.05$ cm$^3$ K mol$^{-1}$, $\theta = 2.5$ K ($T > 15$ K) for **2**, and $C = 1.93$ cm$^3$ K mol$^{-1}$, $\theta = 4.2$ K ($T > 15$ K) for **3**. Since the structural parameters of **2** and **3** around the bridging pathways are relatively analogous as mentioned above, it is possible to directly look into the effect of 4d and 5d magnetic orbitals on magnetic strength. The magnitude of the Weiss constant for **3** is larger than that for **2**, manifesting that the 5d orbital in **3** communicates greater magnetic interactions than the 4d orbital in **2**.[4i] The $M(H)$ data for **2** and **3** were illustrated in Figures 7b and 8b. The ferromagnetic interactions between M(V) and Cu(II) centers via CN bridges are ascertained by the fact that all the data points at the given temperatures stay larger than the theoretical curves. The saturation magnetizations of 5.04 $N\beta$ (**2**) and 5.26 $N\beta$ (**3**) at 7 T are in accordance with the calculated value through the Brilliouin function.

The magnetic properties of **4** were characterized by the temperature and field dependences of magnetic properties, as depicted in Figure 9. The $\chi_m T$ value at 300 K is found to be 1.98 cm$^3$ K mol$^{-1}$, in good agreement with the expected value for isolated two W(V) ($S_W = {}^1/_2$) and three Cu(II) ($S_{Cu} = {}^1/_2$) spins. As observed in **1**−**3**, the $\chi_m T$ product undergoes a continuous and then an abrupt increase, arriving at 5.17 cm$^3$ K mol$^{-1}$ at 2 K. The high-temperature magnetic data comply with the Curie−Weiss equation, giving $C = 1.88$ cm$^3$ K mol$^{-1}$ and $\theta = 15.3$ K ($T > 130$ K). The magnetization per $Cu_3W_2$ increases rapidly with raising field and saturates to a value of 5.01 $N\beta$, which is close to the expected one (5 $N\beta$ with $g = 2$). The experimental curve at 1.9 K is always higher than that derived from the Brillouin function, affirming that the Cu(II) and W(V) spins are ferromagnetically coupled at that temperature.

**Table 2.** Specific Structural Parameters of Axial Cu−$N_{ax}$ Bond Lengths ($d_{Cu-N_{ax}}$) and Related Cu−NC Angles (−Cu−$N_{ax}$−$C_{ax}$) as Well as Weiss Constants ($\theta$) for Octacyanometalate-Based W−Cu Systems Chelated with Tetradentate Macrocycles

| compd | $d_{Cu-N_{ax}}$ (Å) | $\langle d_{Cu-N_{ax}} \rangle$ (Å) | −Cu−$N_{ax}$−$C_{ax}$ (deg) | $\langle$−Cu−$N_{ax}$−$C_{ax}\rangle$ (deg) | $\theta$ (K) | ref |
|---|---|---|---|---|---|---|
| **1** | 2.510−2.698 | 2.588(98) | 143.0−157.1 | 152.4(81) | 1.54 | this work |
| $[Cu(L1)]_3[W(CN)_8]_2 \cdot 6H_2O$ | 2.572−2.607 | 2.593(18) | 137.4−159.2 | 146.9(112) | 3.9 | 17a |
| **3** | 2.494−2.554 | 2.518(32) | 141.1−145.5 | 142.9(23) | 4.2 | this work |
| **4** | 2.371−2.756 | 2.505(158) | 135.7−150.7 | 143.1(55) | 15.3 | this work |
| $[Cu(L4)]_3[W(CN)_8]_2 \cdot 6H_2O_2MeOH$ | 2.409−2.535 | 2.467(64) | 139.4−152.7 | 146.3(67) | 23.0 | 17b |

**Magnetostructural Correlation.** First of all, to understand the fundamental magnetic nature in the present system, a simple orbital scheme is taken into consideration. The magnetic exchange takes place between $Cu^{II}$ ($d^9$) spin residing in $d_{x^2-y^2}$ orbital and $M^V$ [M = Mo ($4d^1$), W ($5d^1$)] spin with $d_{z^2}$ or $d_{x^2-y^2}$ orbitals relying on the geometry around M.[4i,8b,29] The expression of the total exchange coupling constant ($J$) can be equated as $J = J_F$ (ferromagnetic term) + $J_{AF}$ (antiferromagnetic term) = $2k(>0) + 4\beta S(<0)$, where $S$ is the overlap integral.[19] The positive $J$ value would be realized when the $J_F$ component proportional to $k$ is prevalent over $J_{AF}$ dictated by $S$. Hence, if $S$ is quite small or almost zero, $J_{AF}$ becomes negligible with respect to $J_F$ and consequently ferromagnetic coupling ($J > 0$) sets in. It is noticed that all of the prepared Cu−M bimetallic assemblies, which are formed by octacyanometalate(V) and Cu(macrocycle)$^{2+}$, exhibit ferromagnetic interactions between the magnetic centers. These magnetic results demonstrate that, in the light of the given Cu−$N_{ax}$ bond lengths and Cu−N−C angles, a Cu $d_{x^2-y^2}$ magnetic orbital located in the basal plane of the macrocyclic ligand cannot propagate effectively through the empty $\pi^*$ orbital of a CN bridge that overlaps in a $\pi$-pathway with a magnetic orbital ($d_{z^2}$:$d_{x^2-y^2}$) of a M(V) atom. As a result, the overlap ($S$) between magnetic orbitals of Cu(II) and M(V) through the CN bridge is trivial and the sum of $J_F$ and $J_{AF}$ turns to be positive.

To get insight into the magnetic variations related with the Cu−N−C−W bridging paths, the structural data of axial Cu−$N_{ax}$ bond distances ($d_{Cu-N_{ax}}$) and corresponding Cu−$N_{ax}$−$C_{ax}$ angles (−Cu−$N_{ax}$−$C_{ax}$) are scrutinized. As given in Table 2, we focused only on octacyanometalate-based Cu−W bimetallic (3d−5d) complexes to avoid the contribution from disparate d orbitals (4d or 5d) toward magnetic strength.[4i,18] The bond lengths and angles can be tuned by altering side groups attached on macrocyclic ligands. The side groups donate a different degree of steric bulkiness and then have an impact on the structural features around Cu(II) ions. In fact, **1** coordinated by cyclam with no side groups has mostly larger average diatance ($\langle d_{Cu-N_{ax}} \rangle$) and angle ($\langle$−Cu−$N_{ax}$−$C_{ax}\rangle$) than the other complexes possessing macrocyclic ligands with pendant groups. When $d_{Cu-N_{ax}}$ is long enough as in this case, the −Cu−$N_{ax}$−$C_{ax}$ variation across the bimetallic entities appears not to affect the magnetic trait in the current Cu−W systems. In contrast, as $\langle d_{Cu-N_{ax}} \rangle$ diminishes, $\theta$ is prone to be elevated. However, the only parameter considered here is the geometric feature of Cu−NC bond length versus the Weiss constant. The local geometry of the $M(CN)_8$ unit has been shown to have a major effect on the strength of the exchange interaction.[4i] Therefore, the conclusions drawn on the variation of $\theta$ should be tentative.

(29) (a) Hendrickx, M. F. A.; Mironov, V. S.; Chibataru, L. F.; Ceulemans, A. *Inorg. Chem.* **2004**, *43*, 3142. (b) Perumareddi, J. R.; Liehr, A. D.; Adamson, A. W. *J. Am. Chem. Soc.* **1963**, *85*, 249. (c) Burdett, J. K.; Hoffmann, R.; Fay, R. C. *Inorg. Chem.* **1978**, *17*, 2553.

## Conclusions

We have synthesized and characterized four cyano-bridged bimetallic Cu−M (M = Mo, W) compounds specially chelated with diverse macrocyclic ligands. A 1D rope-ladder chain (**1**) was produced when cyclam with no side groups was used, while 2D honeycomb-like structures (**2**−**4**) were isolated in the presence of macrocycles containing pendant groups. The side groups on macrocycles affect variations in apical Cu−$N_{ax}$ lengths and Cu−$N_{ax}$−$C_{ax}$ angles on the bridging pathways. The magnetic comparison between Cu−Mo (3d−4d; **2**) and Cu−W (3d−5d; **3**) complexes with similar structural features clearly shows that 3d−5d magnetic coupling is stronger than 3d−4d because the 5d orbital is more diffuse than 4d. Furthermore, all the compounds display ferromagnetic interactions through CN links under the existent structural parameters. It appears that, on the condition of $d_{Cu-N_{ax}}$ being sufficiently long, the main factor governing the overall ferromagnetic strength concerns the Cu−$N_{ax}$ bond length rather than the Cu−$N_{ax}$−$C_{ax}$ angle.

**Acknowledgment.** This work was supported by a Korea Research Foundation Grant funded by the Korean government (MOEHRD, Basic Research Promotion Fund; Grant KRF-2005-070-C00068) and the Korea Science and Engineering Foundation (KOSEF) grant funded by the Korean government (MOST; Grant R01-2007-000-10240-0).

**Supporting Information Available:** Selected bond distances and angles, additional crystal structures, and crystallographic information (CIF). This material is available free of charge via the Internet at http://pubs.acs.org.

IC701243W